

THE MASS–TO–LIGHT FUNCTION OF VIRIALIZED SYSTEMS AND
THE RELATIONSHIP BETWEEN THEIR OPTICAL AND X-RAY PROPERTIES

CHRISTIAN MARINONI

Department of Astronomy, University of California at Berkeley, Berkeley, CA 94720-3411, US
marinoni@astro.berkeley.edu

MICHAEL J. HUDSON

Department of Physics, University of Waterloo, Waterloo, Canada
mjhudson@astro.uwaterloo.ca

ApJ, submitted

ABSTRACT

We compare the B-band luminosity function of virialized halos with the mass function predicted by the Press-Schechter theory in cold dark matter cosmologies. We find that all cosmological models fail to match our results if a constant mass-to-light ratio is assumed. In order for these models to match the faint end of the luminosity function, a mass-to-light ratio decreasing with luminosity as $L^{-0.5\pm 0.06}$ is required. For a Λ CDM model, the mass-to-light function has a minimum of $\sim 100h_{75}^{-1}$ in solar units in the B-band, corresponding to $\sim 25\%$ of the baryons in the form of stars, and this minimum occurs close to the luminosity of an L^* galaxy. At the high-mass end, the Λ CDM model requires a mass-to-light ratio increasing with luminosity as $L^{+0.5\pm 0.26}$. This scaling behavior of the mass-to-light ratio appears to be in qualitative agreement with the predictions of semi-analytical models of galaxy formation. In contrast, for the τ CDM model, a constant mass-to-light ratio suffices to match the high-mass end.

We also derive the halo occupation number, i.e. the number of galaxies brighter than L_{gal}^* hosted in a virialized system. We find that the halo occupation number scales non-linearly with the total mass of the system, $N_{\text{gal}}(> L_{\text{gal}}^*) \propto m^{0.55\pm 0.026}$ for the Λ CDM model.

We find a break in the power-law slope of the X-ray-to-optical luminosity relation, independent of the cosmological model. This break occurs at a scale corresponding to poor groups. In the Λ CDM model, the poor-group mass is also the scale at which the mass-to-light ratio of virialized systems begins to increase. This correspondence suggests a physical link between star formation and the X-ray properties of halos, possibly due to preheating by supernovae or to efficient cooling of low-entropy gas into galaxies.

Subject headings: cosmology: large-scale structure of the universe — cosmology: dark matter — galaxies: clusters: general — galaxies: halos — galaxies: luminosity function, mass function — X-rays: general

1. INTRODUCTION

One of the major problems of cosmology is to determine the connection between mass and light in the universe over different scales. The abundance by mass of virialized dark matter halos is a fundamental prediction of cosmological models (Press & Schechter 1974). Observationally, halos must be identified with virialized galaxy “systems”, ranging in size from single dwarf galaxies to rich clusters of galaxies.

The masses, and hence the mass multiplicity functions, derived from cataloged systems are not robust, particularly for small systems such as poor groups which contain only a few galaxies. In contrast, halo light is a fundamental observable obeying a robustly determined distribution function, the luminosity function of virialized systems (VSLF).

In a previous paper (Marinoni et al. 2001b, Paper V), we measured the VSLF in the nearby Universe using an objective catalog of virialized systems. In this paper we show how the VSLF can be used to investigate scaling relations between mass and light.

The direct approach to obtaining scaling relations between, for example, mass and light is to regress one parameter on the other. This direct approach has several weaknesses, however. As noted above, for low mass systems

the measured masses can have large errors. Second, the catalogs may be incomplete in either mass or light. Furthermore, it is usually necessary to patch together results from several independent catalogs, each of which probes different mass scales (e.g., galaxies, groups and clusters).

In this paper we take a different approach. We derive the mass functions from theory and compare these with the observed VSLF, solving for the unknown mass-to-light ratio (Υ) as a function of the total mass or luminosity of the halo. The price paid in this approach is that the mass function depends on the assumed cosmological model. The advantage over the conventional approach is that we can simultaneously and seamlessly explore a wide dynamic range in mass and luminosity, free of systematics.

The Υ function, which measures the efficiency with which the universe transforms matter into light, can thus be used not only as a traditional estimator of the density parameter Ω_m but also as a diagnostic tool for different models of galaxy formation.

A closely related statistic, useful in modeling galaxy formation and clustering, is the halo occupation number, i.e. the number of galaxies above some luminosity threshold (chosen to be the absolute magnitude of an L^* galaxy) that populate a virialized halo as a function of its total mass or luminosity.

Within the same framework, we can also investigate the emission properties of halos in different wavelength domains of the electromagnetic spectrum such as in the optical and X-ray bands. The sample of systems for which both the optical and X-ray luminosities are well measured is still limited, and does not allow a reliable determination of the scaling of the X-ray to optical light ratio. However, by comparing statistically their luminosity distributions, we can constrain the functional behavior of this ratio.

This paper is the sixth in a series (Marinoni et al. 1998, Paper I; Marinoni et al. 1999, Paper II; Giuricin et al. 2000, Paper III; Giuricin et al. 2001, Paper IV; Marinoni et al. 2001b, Paper V) in which we investigate the properties of the large-scale structures as traced by the NOG sample. The outline of our paper is as follows: in §2 we review and summarize the determination of the observed luminosity function of virialized halos. In §3 we compare our results with the predictions of τ CDM and Λ CDM models, as well as the predictions from semi-analytic models. In §4, we measure the halo occupation number. In §5 we examine the relationship between the optical and X-ray properties in virialized systems. In §6 we discuss in detail the resulting scaling relations between the properties of groups and clusters of galaxies. Results are summarized in §7.

Throughout this paper, the Hubble constant is taken to be $75 h_{75} \text{ km s}^{-1} \text{ Mpc}^{-1}$ and the recession velocities cz_{LG} are evaluated in the Local Group rest frame.

2. THE LUMINOSITY FUNCTION OF VIRIALIZED HALOS

In paper V, we determined the luminosity function of virialized systems using groups extracted from the NOG galaxy catalog. The NOG sample (Marinoni 2001a) is a statistically controlled, distance-limited ($cz_{\text{LG}} \leq 6000 \text{ km s}^{-1}$) and magnitude-limited ($B \leq 14$) complete sample of more than 7000 optical galaxies. The sample covers $2/3$ (8.27 sr) of the sky ($|b| > 20^\circ$), a volume of $1.41 \times 10^6 h_{75}^3 \text{ Mpc}^{-3}$ and has a redshift completeness of 98%.

From the NOG, three different “virialized system” samples were determined using groups selected by three different objective group-finding algorithms (Paper III). In paper V, we showed that the VSLF derived from these different samples are consistent and hence that the VSLF is robust.

In order to recover accurately the absolute luminosity of a given halo, we correct for both the integrated luminosity of galaxies below the magnitude limit of the sample and for the completeness of subsamples of the halo catalog. Moreover, models to correct for the large-scale motions (Paper I) have been applied in order to improve the determination of the halo distances. The key steps of the reconstruction procedure are shown in Fig. 1, focusing on several virialized systems in the Virgo region which are embedded in lower-density filamentary large-scale structure.

In Paper V, we found that the B -band luminosity function of the whole hierarchy of gravitationally bound systems, from single galaxies to rich clusters, was insensitive to the choice of the group-finding algorithms with which halos are selected, and was well described over the absolute-magnitude range $-24.5 \leq M_s + 5 \log h_{75} \leq -18.5$ by a Schechter function (Schechter 1976) with $\alpha_s = -1.4 \pm 0.03$, $M_s^* - 5 \log h_{75} = -23.1 \pm 0.06$ and $\phi_s^* =$

$4.8 \times 10^{-4} h_{75}^3 \text{ Mpc}^{-3}$ or by a double power law: $\phi_{\text{pl}}(L_s) \propto L_s^{-1.45 \pm 0.07}$ for $L_s < L_{\text{pl}}$ and $\phi(L_s) \propto L_s^{-2.35 \pm 0.15}$ for $L_s > L_{\text{pl}}$ with $L_{\text{pl}} = 8.5 \times 10^{10} h_{75}^{-2} L_\odot$, corresponding to $M_s - 5 \log h_{75} = -21.85$. The characteristic luminosity of virialized systems, L_{pl} , is ~ 3 times brighter than that (L_{gal}^*) of the luminosity function of NOG galaxies.

3. THE MASS-TO-LIGHT RATIO OF VIRIALIZED SYSTEMS

3.1. Introduction

In order to compare observational data with theoretical predictions, the traditional approach has been to estimate the halo mass of groups and clusters directly from the data, using, for example, velocity dispersions of galaxy members (Carlberg et al. 1996; Girardi et al. 1998), X-ray gas temperatures (David, Jones, & Forman 1996; Lewis et al. 1999), and gravitational lensing (Smail et al. 1997, Allen 1998).

The application of these methods is reasonably straightforward for rich clusters of galaxies but is more problematic for poor groups, due to their low X-ray surface brightness and the poor sampling of optical dynamical mass estimators (see, e.g., Zabludoff & Mulchaey 1998, Mahdavi et al. 1999). Consider, for example, a system composed of a few elements selected from a magnitude-limited survey. In this case one will miss faint members that do not satisfy selection criteria. The contribution of faint members to the total luminosity of the system is negligible small, and can easily be corrected (see Paper V). In contrast, these faint galaxies are important dynamical probes of the gravitational potential well, and their omission can translate into a serious bias in the estimated mass, particularly if galaxies of different luminosities are clustered in different ways (Park et al. 1994; Giuricin et al. 2001). Moreover one can construct a completeness function and then derive a differential distribution function for the light emitted by virialized systems, while the construction of a similar completeness function involving dynamical estimators (velocity dispersion for example) is very problematic (Borgani et al. 1997). Thus, the luminosity function of virialized systems is more robust on group scales than is the mass function derived using projected velocity dispersions.

In this paper, following Cavaliere, Colafrancesco & Scaramella (1991) and Moore, Frenk, & White (1993, MFW), we explore an alternative approach to determining the mass-to-light ratio over a range of scales including both poor and rich systems. Specifically, we compare the robust observationally-determined luminosity function of systems to theoretically-determined mass functions.

3.2. Theory

The differential mass function of virialized systems $n(m)$ can be calculated, for a given cosmological model, via the Press-Schechter formalism (Press & Schechter 1974, hereafter PS; Schaeffer & Silk 1985; Bower 1991; Bond et al. 1991; Cavaliere, Colafrancesco, & Scaramella 1991; Lacey & Cole 1993; Monaco 1998), or more accurately, through N-body simulations (Efstathiou & Rees 1988; Lacey & Cole 1994; Governato et al. 1999; Jenkins et al. 2001). The comparison with N-body simulations reveals that the PS mass function provides a reasonably accurate description of the abundance of virialized halos on group and cluster scales although it tends to overpredict

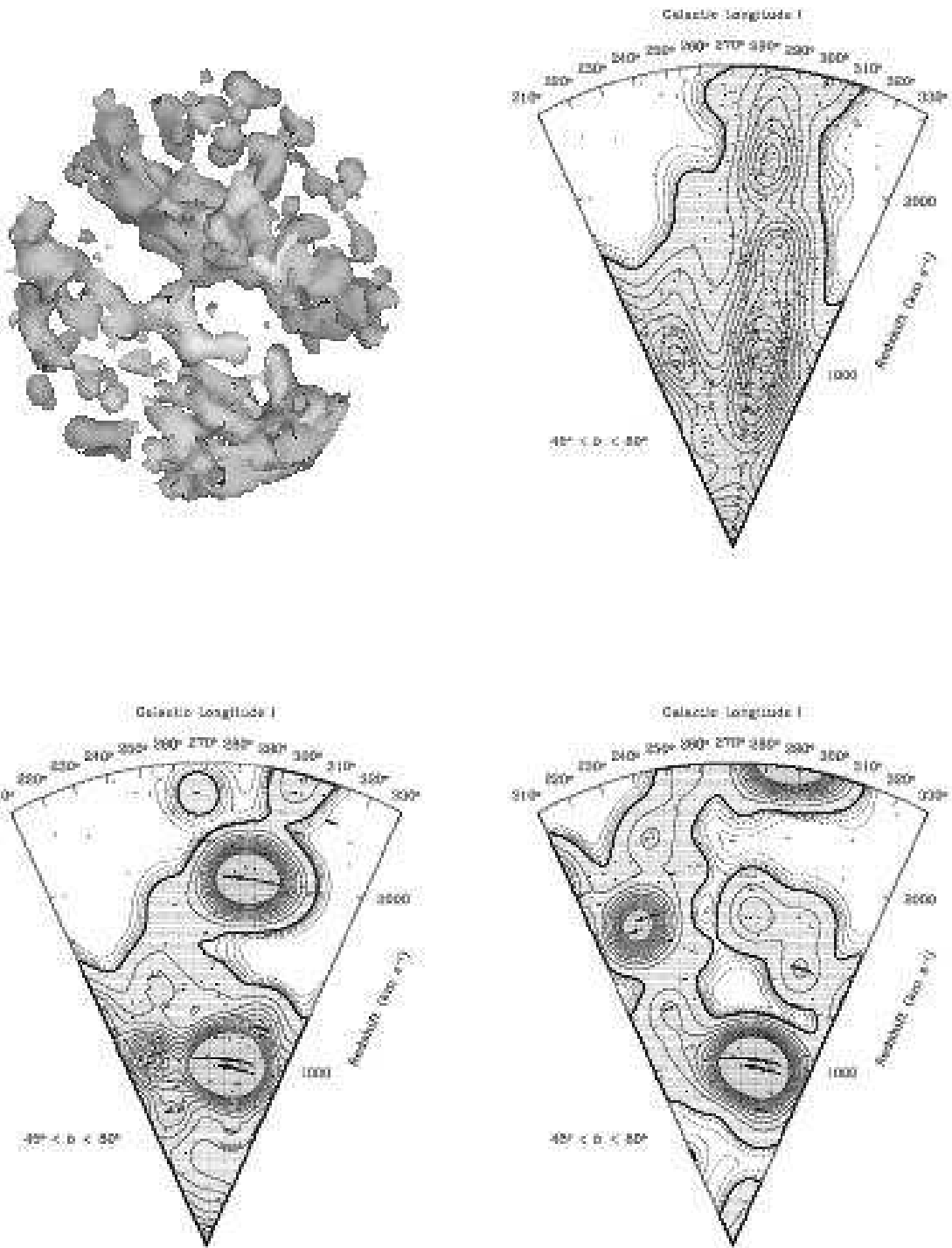


FIG. 1.— *Upper left*: Density ($\delta=1.5$) distribution of NOG galaxies smoothed using a Gaussian window function with smoothing length $R_s = 200 \text{ km s}^{-1}$. *Upper right*: redshift distribution of NOG galaxies in a cone diagram centered on the Virgo region (smoothed with $R_s = 100 \text{ km s}^{-1}$). Regions with $\delta > 0$ are in grey scale while contours are spaced by $\Delta\delta = 2$. *Lower left*: the same region after clustering reconstruction with the hierarchical method. (*Lower right*: the same region after having applied the peculiar velocity field model fitted using Mark III data.

(albeit by a small amount) the abundance of low-mass halos and underpredict that of high-mass halos (e.g., Gross et al. 1998; Sheth & Tormen 1998; Governato et al. 1999). Given the uncertainties in the luminosity function of systems to which we will be comparing the mass function, the PS formula is of sufficient accuracy.

The PS analytical expression for the present-day comoving number density of dark halos of mass m in the interval dm is

$$n(m)dm = \sqrt{\frac{2}{\pi}} \frac{\bar{\rho}\delta_c}{\sigma(m)^2 m} \exp\left(-\frac{\delta_c^2}{2\sigma(m)^2}\right) \left(\frac{d\sigma(m)}{dm}\right) dm \quad (1)$$

where $\bar{\rho}$ is the present mean density of the universe, $\sigma(m)$ is the present-day *rms* fluctuations of the linear density field after smoothing with a spherical top-hat filter containing a mean mass m (and it is specified by the power spectrum, $P(k)$, of the density fluctuations), and δ_c is a density threshold usually taken to be the extrapolated linear overdensity of a spherical perturbation at the time it collapses. The parameter δ_c is only weakly-dependent on matter density parameter Ω_m and the cosmological constant Ω_Λ (varying by less than 0.02 for flat models with $\Omega_m > 0.1$, see Fig. 1. of Eke, Cole, & Frenk 1996), and so has been set to its Einstein-de Sitter cosmology value 1.686.

The dimensionless power spectrum ($\Delta(k) \equiv V(2\pi^2)^{-1}k^3|\delta_k|^2$ in the linear regime is given by the analytic approximation of Bond & Efstathiou (1984)

$$\Delta(k) = \frac{Ak^4}{\left[1 + [aq + (bq)^{3/2} + (cq)^2]^\nu\right]^2} \quad (2)$$

where $q = k/\Gamma$, $a = 6.4h_{100}^{-1}$ Mpc, $b = 3h_{100}^{-1}$ Mpc, $c = 1.7h_{100}^{-1}$ Mpc, $\nu = 1.13$, and $h_{100} = H_0/(100 \text{ km s}^{-1} \text{ Mpc}^{-1})$. The parameter $\Gamma = \Omega_m h_{100}$ (if we neglect the effect of baryons) determines the shape, and the normalization is determined e.g. by Cosmic Microwave Background fluctuations or by fixing the *rms* fluctuations on a scale of $8h_{100}^{-1}$ Mpc, σ_8 .

3.3. Results

Figure 2 shows the PS-predicted luminosity functions obtained assuming constant mass-to-light ratio for four different cosmological models: Standard CDM ($\Omega_m = 1$, $\Omega_\Lambda = 0$, $H_0 = 50 \text{ km s}^{-1} \text{ Mpc}^{-1}$, $\sigma_8 = 0.51$), Λ CDM ($\Omega_m = 0.3$, $\Omega_\Lambda = 0.7$, $H_0 = 70 \text{ km s}^{-1} \text{ Mpc}^{-1}$, $\sigma_8 = 0.9$), τ CDM ($\Omega_m = 1$, $H_0 = 50 \text{ km s}^{-1} \text{ Mpc}^{-1}$, $\sigma_8 = 0.51$, $\Gamma = 0.21$) and Open CDM ($\Omega_m = 0.3$, $\Omega_\Lambda = 0$, $H_0 = 70 \text{ km s}^{-1} \text{ Mpc}^{-1}$, $\sigma_8 = 0.85$). These models are described in detail by Jenkins et al. (1998) and are normalized adopting the values for the fluctuations in an $8 h_{100}^{-1}$ Mpc sphere, σ_8 , prescribed by Eke, Cole, & Frenk (1996) from their analysis of the local cluster X-ray temperature function.

The NOG VSLF and the corresponding MFW results are shown in Figure 2. The latter is represented by a hatched region, which shows how the VSLF varies if the overdensity contrast used in identifying groups is varied from 50 to 300.

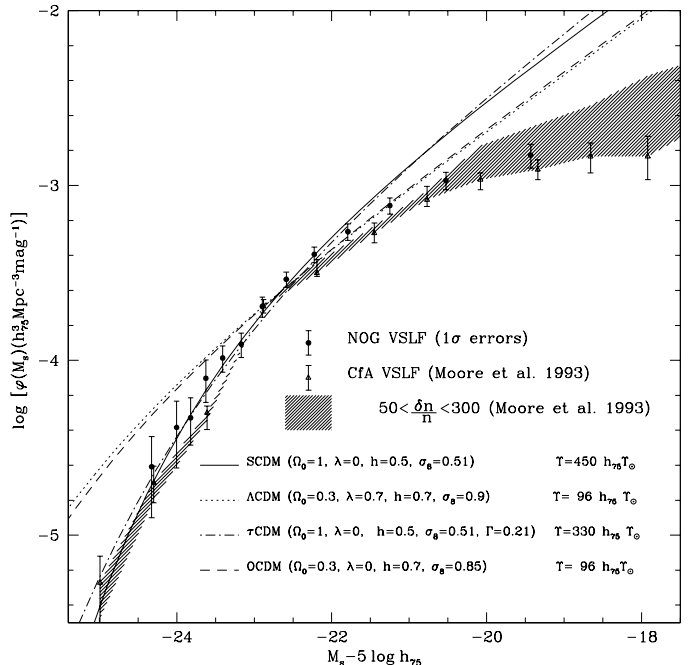


FIG. 2.— The NOG and CfA system LFs are compared with the luminosity distribution predicted using the Press-Schechter function and a constant mass-to-light ratio. Four different cosmological models (the standard CDM, Λ CDM τ CDM and open CDM) are computed with cosmological parameters as given in the figure. For each model we show the constant mass-to-light ratio adopted. The hatched region indicates how the LF varies if the overdensity criterion $\frac{\delta n}{n}$ used in identifying groups is varied from 50 to 300.

The friends-of-friends grouping algorithm used to define the groups and hence the VSLF requires that the local density contrast at the edge of a group be greater than some limiting threshold $\frac{\delta n}{n}$ (see the discussion in §2). If we assume a spherical halo with a singular isothermal density profile $n(r) \propto r^{-2}$, this local density threshold corresponds to a mean overdensity $\langle \frac{\delta n}{n} \rangle = 3 \frac{\delta n}{n}$ where the average is performed over the typical separation of group members (virialization region). Thus, if galaxy biasing is negligible, for our grouping algorithms, this implies a value which is close to the mean overdensity of nearly 180 predicted for a top-hat spherical collapse in the case of $\Omega_m = 1$ (see Eke, Cole, & Frenk 1996 for values in different cosmologies).

Cole & Lacey (1996) found that the virialized regions of N-body halos are reliably identified using the percolation method and a local density threshold parameter of nearly 60. Using this limiting density contrast, they are able to reproduce the bulk properties of virialized structures (in particular the virial mass) and concluded that the closeness to global virial equilibrium of the identified N-body halos depends rather weakly on the adopted limiting threshold. Moreover, as noted by Diaferio et al. (1999), the average luminosities of groups objectively identified from a redshift survey with typical *friends-of-friends* parameters are in agreement with those of groups extracted from real-space simulations. Thus, we can use our VSLF for a meaningful comparison with the PS predictions.

Figure 2 indicates that, in agreement with previous results, all models fail to describe the observed faint-end slope.

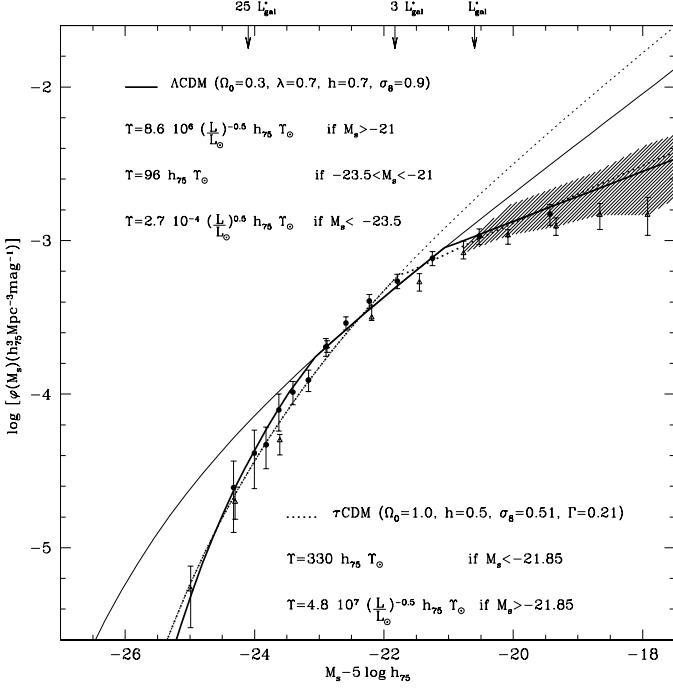


FIG. 3.— The NOG and CfA system LFs are compared with the luminosity distribution predicted using the Press-Schechter function. The LF in the τ CDM and Λ CDM scenarios are computed for constant mass-to-light ratios ($\Upsilon = 330h_{75}\Upsilon_{\odot}$ and $\Upsilon = 96h_{75}\Upsilon_{\odot}$ respectively) and also (heavy lines) using the piecewise mass-to-light ratios given in the figure. The hatched region indicates how the LF varies if the overdensity criterion $\frac{\delta n}{n}$ used in identifying groups is varied from 50 to 300.

More interestingly, several models (Λ CDM and τ CDM) fail to reproduce the bright end of the LF, if a constant mass-to-light ratio is assumed.

We can turn this problem around, and solve for the mass-to-light function, $\Upsilon(m)$, required to fit the observed VSLF. We assume that there is a monotonic relation between the mass and light of virialized systems, i.e. $L_s = f(m)$ with no scatter.

It is possible to obtain an exact numerical solution by noting that the Υ function is defined implicitly by the requirement that the number density of systems above with masses greater than mass m must be the same as the number density of systems with luminosities greater than $L_s = f(m)$,

$$N_s[> L_s = f(m)] = N_s(> m) \quad (3)$$

where $N_s(> L_s)$ is given by the appropriate integral over the VSLF

$$N_s(> L_s) = \int_{L_s}^{\infty} \phi(L_s) dL_s \quad (4)$$

and $N_s(> m)$ is the corresponding integral over the PS mass function.

The LF integral can be obtained analytically, but the PS mass function integral must be solved numerically. The mass-to-light ratio is then given by

$$\Upsilon = \frac{m}{f(m)} \quad (5)$$

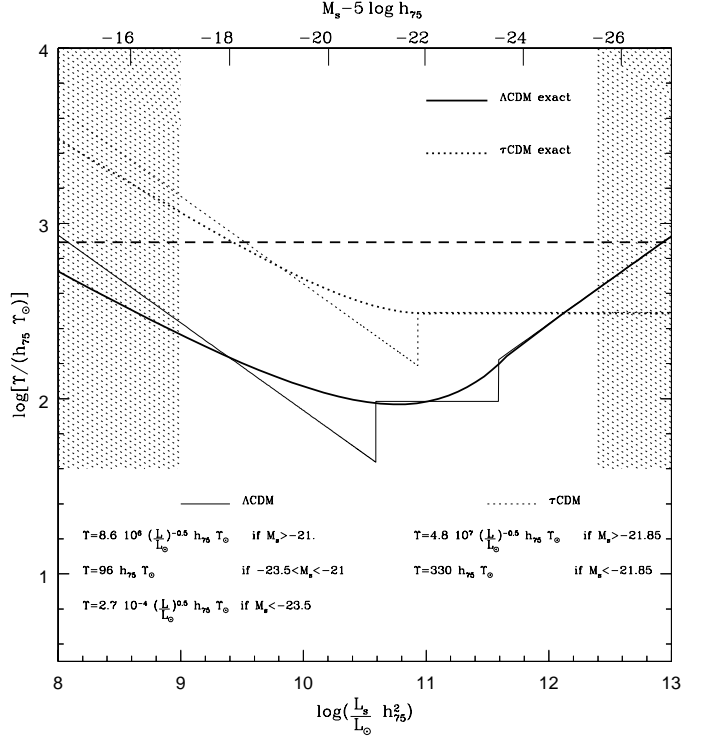


FIG. 4.— Mass-to-light ratio as a function of luminosity for the Λ CDM and τ CDM models. The thin solid and dotted lines indicate the mass-to-light ratios for the piecewise models shown in Fig. 3 for the Λ CDM and τ CDM models respectively, whereas the thick lines are the exact solutions obtained by solving eq. 3. The dashed line indicates the critical value of the mass-to-light ratio. The hatched region represents extrapolation to regions not covered by our data.

If we assume that mass and light are simply related via a power law expression $\Upsilon \propto L_s^\gamma$, the halo luminosity function assumes the simple analytical form

$$\phi(M_s) \propto mn(m)(1 + \gamma) \quad (6)$$

The predicted VSLFs obtained fitting “piecewise” Υ functions are shown in Figure 3 for the τ CDM and Λ CDM models, which are used here as our reference models.

In Table 2, we give the masses assigned to luminous systems for the numerical solution of the Υ function. In Figure 4, the piecewise and numerical solutions for Υ are plotted as a function of luminosity. The result is that, for both models, Υ must go approximately as $L_s^{-0.5 \pm 0.06}$ on small scales. Interestingly, this behavior agrees with the direct determinations of Υ derived for spiral galaxies from the analysis of their rotation curves and for ellipticals from a variety of tracers of galactic gravitational field (see the review by Salucci & Persic 1997).

The Υ function reaches a minimum at a luminosity of approximately $10^{10.5} h_{75}^{-2} L_{\odot}$, which corresponds roughly to L_{gal}^* . Then it remains quite flat over ~ 1 dex in luminosity. The behavior at the bright end is model-dependent: for the τ CDM model, Υ must remain constant ($m \propto L_s^{1 \pm 0.1}$), whereas for the Λ CDM model it must increase with luminosity as $L_s^{0.5 \pm 0.26}$ from the scale of galaxy groups ($m \sim 10^{13} m_{\odot} h_{75}^{-1}$) to that of rich clusters ($\sim 10^{15} m_{\odot} h_{75}^{-1}$).

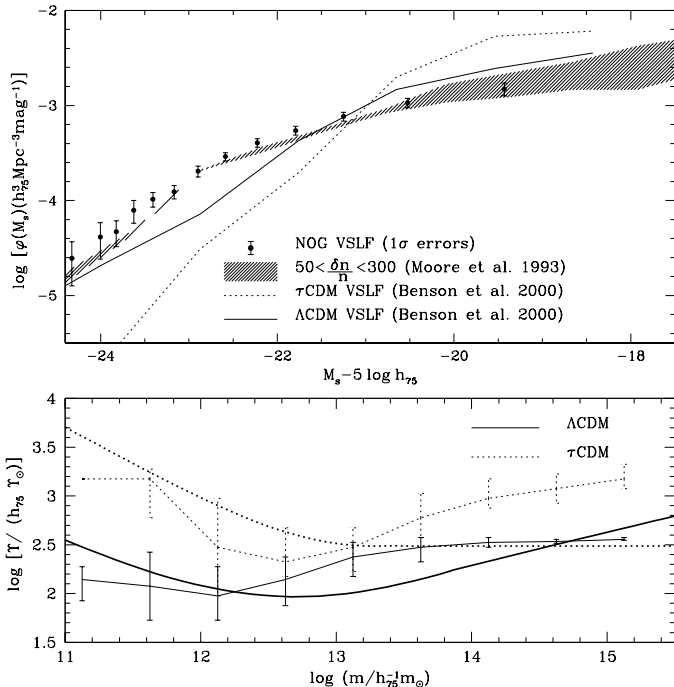


FIG. 5.— *Upper*: the NOG VSLF (points with $\pm 1\sigma$ error bars) is shown in comparison with the semi-analytic prediction of Benson et al. (2000). Results from their τ CDM and Λ CDM models are plotted with short-dashed lines and solid lines respectively. *Lower*: mass-to-light ratios from Fig. 4 (smooth curves) are compared to those derived by Benson et al. (curves with error bars).

Recall that our mass-to-light ratios are based on the PS mass functions. If, as mentioned above, the PS prescription underestimates the abundance of high-mass objects, the true scaling at the high-luminosity end is likely to be somewhat steeper than found above. This would also be true if we used a lower value $\delta_c = 1.3$ in the PS mass function, as might be expected for a non-spherical collapse for bound structures.

3.4. Discussion

It is interesting to compare the Υ functions derived in the previous subsection with values found via direct mass estimates. As discussed above, these direct methods are problematic for low mass systems such as single galaxies (because the full extent of the dark matter halo is not probed) or poor groups (because of the small numbers of dynamical test particles). The Υ values found in the literature are consistent with the range $\sim 100h_{75}\Upsilon_{\odot}$ to $\sim 300h_{75}\Upsilon_{\odot}$ spanned by the Λ CDM and τ CDM models considered here.

For high masses, we can compare our results with the scaling behavior of Υ obtained via direct determinations of the virial masses of galaxy clusters. Schaeffer et al. (1993) found that $\Upsilon_V \propto L_V^{0.3}$. Girardi et al. (2000) analyzed 105 rich clusters and found $\Upsilon_{B_j} \propto L_{B_j}^{0.2-0.3}$.

They also noted that a variation of Υ with scale could not be explained by a higher fraction of spirals in poorer clusters, thus suggesting that a similar result would also be found by using R-band galaxy magnitudes. Carlberg et al. (1996) found that the number of bright galaxies per unit mass is systematically lower in cluster with higher ve-

locity dispersion. This result would imply that Υ increases with cluster mass, if the shape of the luminosity function of cluster galaxies were independent of cluster mass.

These results are in agreement with the mass-to-light function of the Λ CDM model, but not with that of the τ CDM model.

On the largest scales, the behavior of the mass-to-light function is less clear. Virialized objects of supercluster mass are expected to be extremely rare — there are certainly none in the NOG volume. It is possible to obtain direct estimates of the global mass-to-light ratio can obtained from studies of peculiar velocities, which probe deviations from the uniform expansion of the Universe. Note that the peculiar velocity of a given galaxy is generated by a large number of massive halos over a range of distances, in both overdense and underdense regions. Thus the mass-to-light ratio determined by such studies is an average over a range of mass scales. Hudson (1993, 1994) studied the density field and peculiar velocity field in a volume very similar to the NOG. He assumed a constant mass-to-light ratio for all systems and found that the average mass-to-light ratio of optical galaxies was 30% of the mass-to-light ratio of a critical density Universe, if galaxies are unbiased tracers of the mass. It would be interesting to see how these conclusions would be altered if one adopted the mass-to-light function found here for the Λ CDM model.

Our results can also be used to determine the efficiency of star formation, namely the fraction of all baryonic material which has turned into stars. We can convert our Υ function into a stellar-to-total mass ratio if we assume a stellar mass-to-light ratio averaged over spheroids and disks, of $\Upsilon_{\text{star}} = 3.4\Upsilon_{\odot}$ (Fukugita, Hogan & Peebles, 1998) in the B -band. Near the minimum of the Υ function, this yields a mass fraction of stars, $M_{\text{star}}/M_{\text{tot}} \sim 0.035h_{75}^{-1}$. The mass fraction in stars can then be converted into the fraction of baryons in stars, if we assume that the baryonic-to-total mass fraction in virialized systems is the same as the global value, $\Omega_{\text{baryon}}/\Omega_{\text{m}}$. Using $\Omega_{\text{baryon}} = 0.022h_{100}^{-2}$ from Netterfield et al. (2001), we obtain the stellar-to-baryonic fraction

$$M_{\text{star}}/M_{\text{baryon}} \sim 0.26 \left(\frac{\Upsilon}{100h_{75}\Upsilon_{\odot}} \right)^{-1} \left(\frac{\Omega_{\text{m}}}{0.3} \right) h_{75} \quad (7)$$

Thus in those dark matter halos which have luminosities in the range $1 - 10L_{\text{gal}}^*$, masses in the range $10^{12} - 10^{13}m_{\odot}$ and where $\Upsilon \sim 100h_{75}\Upsilon_{\odot}$, $\sim 25\%$ of the mass is converted into stars. This is considerably more efficient than the global stellar fraction of $\lesssim 10\%$ (Fukugita et al. 1998).

For the Λ CDM model, the mass-to-light-ratio increases to $\Upsilon = 350h_{75}\Upsilon_{\odot}$ at cluster masses $\sim 5 \times 10^{14}h_{75}^{-1}m_{\odot}$. At this mass, the star formation efficiency has dropped to 7.4%. If we also allow for the redder population of such systems, and assign a higher stellar $M/L_B = 4.5$ (Fukugita et al. 1998), the star formation efficiency would be 10%. This is in agreement with the results of Balogh et al. (2001). For the τ CDM model, the mass-to-light ratio is $\sim 330h_{75}\Upsilon_{\odot}$ for all systems with masses greater than $10^{13}h_{75}^{-1}m_{\odot}$, and in this mass range the star formation efficiency would be $\sim 25\%$.

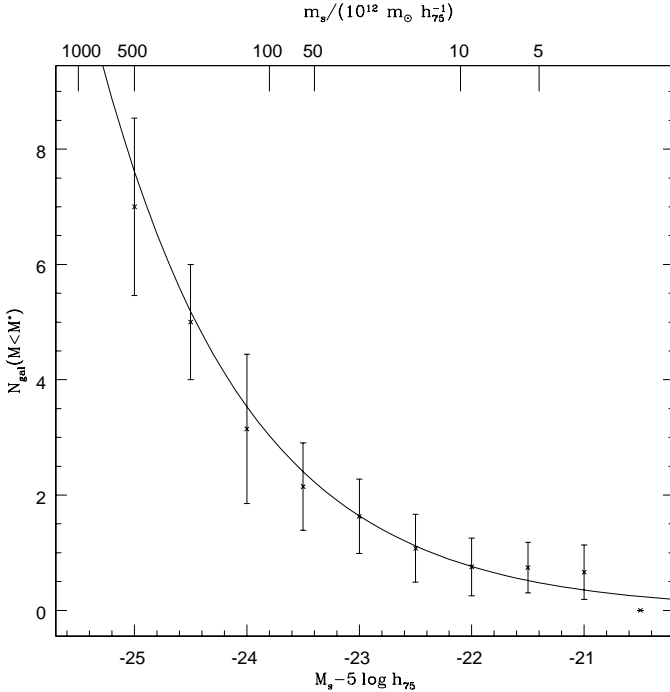


FIG. 6.— The number of galaxies with luminosity greater than L_{gal}^* hosted in a halo is plotted as a function of the system luminosity. Bars represent $\pm 1\sigma$ errors calculated as the standard deviation in each bin of absolute magnitude. The mass scale is obtained using the mass-to-light ratio derived in a Λ CDM cosmogony in §4. Also shown the best fitting curve as determined in equation refnl.

Finally, we can compare our VSLF to the predictions of semi-analytic models, such as those of Benson et al. (2000). In Figure 5, we show our LF and that of MFW in comparison with the predictions of their Λ CDM and τ CDM models. Benson et al. constrained their models to match the amplitude of the ESP galaxy LF in the B_J -band (Zucca et al. 1997) at their L_{gal}^* . Their τ CDM model is quite a poor fit, failing to match the slope of our VSLF at intermediate luminosities and predicting too many low-luminosity objects. Their Λ CDM model provides a marginal fit to our results: the bright-end slope is correct, although the predicted LF slope in the range of groups is somewhat too steep. This arises because their Υ function increases as $m^{0.3}$ between masses of $10^{12}m_{\odot}$ and $10^{14}m_{\odot}$, whereas we find that the behavior of Υ is quite flat in this range (see Fig. 4). An increase in Υ from the scales of large galaxies up to clusters is also predicted by the galaxy formation models of Kauffmann et al. (1999), with $\Upsilon_B \propto m^{0.2}$ over the range $10^{12}m_{\odot} < m < 10^{15}m_{\odot}$ for both their Λ CDM and τ CDM models. This is similar to that found by Benson et al., and suggests that the Kauffmann et al. VSLF would be qualitatively similar to that of Benson et al. The Υ functions obtained from the semi-analytic models of Somerville et al. (2001) also increase with increasing mass, however their Υ values are larger than those of Benson et al. and are thus in poorer agreement with those derived here.

4. HALO OCCUPATION NUMBERS

For many purposes, it is important to know the *number* of galaxies which populate a given halo. Once this function

is known, one can use the well-understood clustering of halos to obtain the clustering of galaxies (Neyman, Scott and Shane 1953; Kauffmann et al. 1999; Diaferio et al. 1999; Benson et al. 2000; Seljak 2000; Peacock and Smith 2000; Scoccimarro et al. 2001; Benson 2001).

In Fig. 6, we plot the number of galaxies with luminosity greater than L_{gal}^* as a function of the corrected halo luminosity and of the total halo mass derived under the assumption of a Λ CDM cosmogony (§3). Note that NOG sample is complete for $L_{\text{gal}} > L_{\text{gal}}^*$ (see Fig. 6 of Paper V) and no luminosity selection effects are polluting the observed trend. Note that, by definition, we are only considering the high-luminosity ($L_{\text{gal}} > L_{\text{gal}}^*$) end of the Υ function. We find that the number of galaxies above the L_{gal}^* luminosity threshold, scales with the total luminosity of the system as follows

$$N_{\text{gal}}(> L_{\text{gal}}^*) = (0.26 \pm 0.02) \left(\frac{L_s}{L_{\text{gal}}^*} \right)^{0.83 \pm 0.25}, \quad (8)$$

for $M_s - 5 \log h_{75} < -21$. Using the mass-to-light ratio derived in section §3 we can derive the dependence of the number of objects residing within halos in terms of the halo mass and of the specific cosmological model adopted. We find that in a Λ CDM and τ CDM cosmogonies, the scaling of the halo occupation number with mass is given by the following expressions

$$N_{\text{gal}}(> L_{\text{gal}}^*) = 6.3 h_{75}^{4/3} \cdot 10^{-8} \left(\frac{m}{m_{\odot}} \right)^{0.55 \pm 0.26} \quad (9)$$

for $m \gtrsim 5 \times 10^{12} h_{75}^{-1} m_{\odot}$ and

$$N_{\text{gal}}(> L_{\text{gal}}^*) = 4.2 h_{75} \cdot 10^{-12} \left(\frac{m}{m_{\odot}} \right)^{0.83 \pm 0.33} \quad (10)$$

for $m \gtrsim 10^{13} h_{75}^{-1} m_{\odot}$, respectively.

Peacock and Smith (2000) performed a similar analysis using CfA (Ramella, Pisani & Geller 1997) and ESO Slice Project groups (Ramella et al. 1999). Their Figure 6 suggests power-law exponents of ~ 0.55 and ~ 0.7 , for Λ CDM and τ CDM models respectively, in good agreement with our results.

5. THE RELATION BETWEEN OPTICAL AND X-RAY PROPERTIES IN VIRIALIZED SYSTEMS

Having derived the functional form of the optical luminosity distribution of virialized systems, we now investigate the relation between optical and X-ray emission properties in galaxy systems. The techniques involved are the same as those developed in section §2. The general problem of deriving the functional form $L_X = f(L)$, relating the optical and the X-ray luminosities, can be formulated using the following differential equation

$$\begin{cases} \mathcal{L}_X = f(\mathcal{L}_s) \\ \frac{df(L_s)}{dL_s} = \frac{\phi(L_s)}{\phi(L_X)} \end{cases} \quad (11)$$

where $\phi(L_s)$ is the optical LF of systems emitting in the X-ray band with a luminosity distribution $\phi_X(L_X)$, and where $\mathcal{L}_X = f(\mathcal{L}_s)$ is the initial condition, which can be determined from the data.

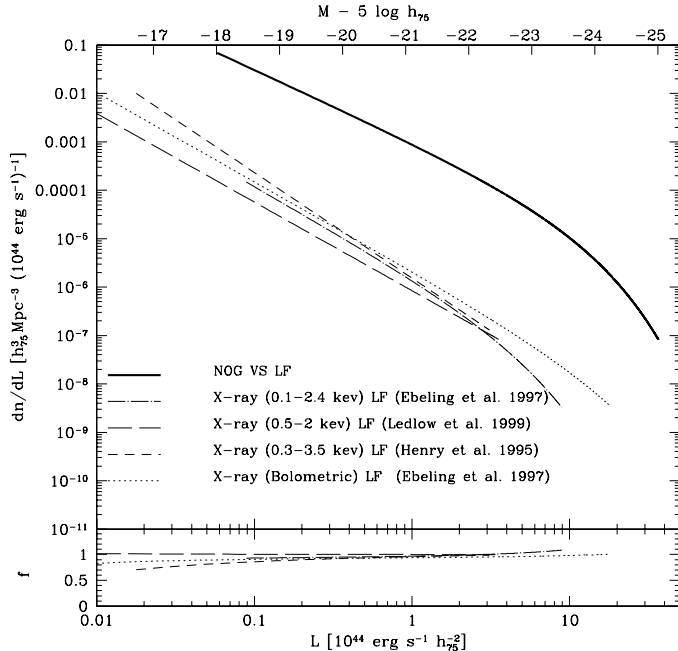


FIG. 7.— *Upper*: the local X-ray luminosity functions in four different bands are compared over a luminosity range that describes both groups (faint end) and clusters (bright end). The shape of the NOG VSLF is shown for comparison. *Lower*: the ratio f between the logarithms of the four X-ray luminosity functions and a power law expression of parameters $\alpha_X = -1.85$ and $\phi_X^* = 4 \cdot 10^{-7} \text{Mpc}^{-3} (10^{44} \text{ergs}^{-1})^{\alpha_X - 1}$ is shown as a function of luminosity.

We assume that all virialized systems detected in the optical also radiate in X-rays. Their optical LF is a Schechter function whose parameters ($\phi_s^*, \alpha_s, M_s^*$) are known over the luminosity range $-18 < M_s - 5 \log h_{75} < -25$ (§3 and Fig. 7). The XLFs in various bands are given by Ebeling et al. (1997).

The optical emission is expected to be connected with the X-ray emission under the standard assumption that the same gravitational potential shapes the gas density distribution as well as the galaxy distribution (Cavaliere & Fusco-Femiano 1976). We can gain some insights into the optical-to-X-ray luminosity ratio making some approximations. Fig. 7 shows that $\phi_X(L_X)$, for both groups and clusters, can be well approximated, in almost all the X-ray bands, by a single power-law expression $\phi_X(L_X) = \phi_X^* L^{\alpha_X}$. In particular, in the bolometric and 0.1-2.4 keV bands, the local XLFs of Ebeling et al. (1997) are very well approximated (and extrapolated into the group domain) by the following fitting parameters $\phi_X^* \sim 4 \cdot 10^{-7} \text{Mpc}^{-3} (10^{44} \text{erg s}^{-1})^{\alpha_X - 1}$ and $\alpha_X \sim 1.85$. In this case, the particular solution of eq. 11 is simple and can be expressed by the following analytical formula

$$L_X = \left\{ f(L_s)^{\beta_X} - C \beta_X \left[\Gamma_i \left(\beta_s, \frac{L_s}{L_*} \right) - \Gamma_i \left(\beta_s, \frac{L_s}{L_*} \right) \right] \right\}^{\frac{1}{\beta_X}} \quad (12)$$

where $C = \phi_s^* / \phi_X^*$, $\beta = 1 + \alpha$ (for s and X subscripts) and Γ_i is the incomplete gamma function. However, if we integrate numerically the differential equation 11, we obtain the result plotted in Fig. 8.

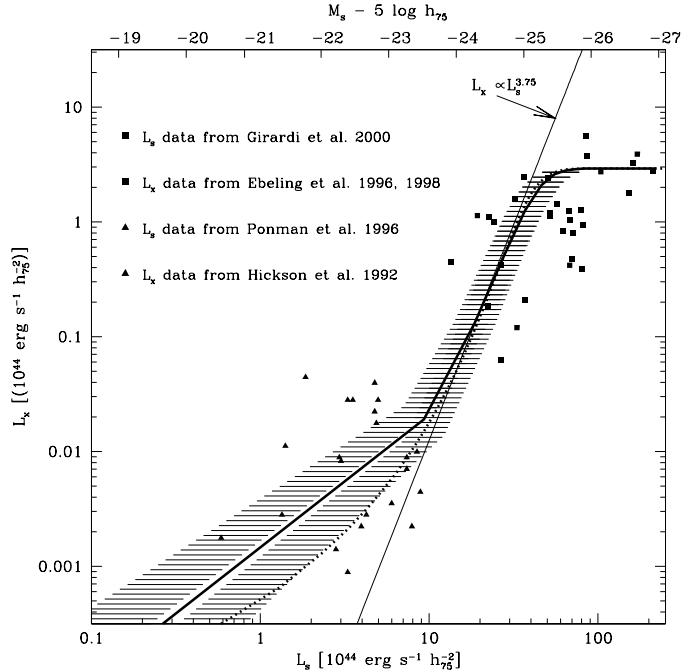


FIG. 8.— The relation between optical (L_s) and X-ray (L_X) luminosities as determined in eq. 12 is shown together with the observed luminosities of Abell clusters. The straight line is the scaling relation predicted in a Λ CDM universe using the optical (this paper) and the X-ray (Ledlow et al. 1999) mass-to-light ratios with arbitrary normalization. The thick solid line is the exact solution and the dotted line is the analytical solution of eq. 12. The hatched region corresponds to the errors in the $L_X - L_s$ relation obtained from the errors in the respective luminosity functions.

In order to test the solution and determine the normalization constant, we have used a sample of Abell clusters for which both the optical blue magnitudes and the X-ray luminosities in the 0.1-2.4 keV band are known. The largest local samples of X-ray luminosities compiled to date are the X-ray Brightest Abell Cluster Sample XBACS (Ebeling et al. 1996) and the Brightest Cluster Sample (BCS) (Ebeling et al. 1998). We found that 28 XBACS and 3 BCS clusters also have estimated B_J luminosities (Girardi et al. 2000). At the low-luminosity end we used a sample of compact groups whose luminosities in the X-ray (bolometric) and optical (blue) passbands are given by Ponman et al. (1996) and Hickson et al. (1992) respectively. In order to reduce observational errors, the initial condition has been determined by averaging the luminosities of the four optically brightest clusters in the sample.

The overall agreement between our prediction and the data is shown in Fig. 8. Note that the Girardi et al. (2000) data shown here are at the tail of our optical VSLF. Of particular interest is the apparent break in the power-law behavior at $M_s = -21 + 5 \log h_{75}$, $L_X \sim 10^{42} \text{erg s}^{-1} h_{75}^{-2}$. Fainter than this break, the numerical solution is well approximated by $L_X \propto L_s^{1.5}$, whereas in the brighter regime, both numerical and analytic solutions are well approximated by $L_X \propto L_s^{3.5}$.

When considering X-ray properties, as well as mass-to-light ratios, it is convenient to separate poor systems, by which we mean systems with one or a few L_{gal}^* galaxies (poor groups), from rich systems (rich groups and clusters). We define the former to be those systems with $-21 > M_s - 5 \log h_{75} > -23$ or $L_X < 10^{42} \text{ erg s}^{-1} h_{75}^{-2}$, and the latter to be systems with $-23 > M_s - 5 \log h_{75} > -25$ or $10^{42} < L_X / (\text{erg s}^{-1} h_{75}^{-2}) < 5 \cdot 10^{44}$. Beyond this range the X-ray and optical LFs are not well determined from our data

6.1. Scaling relations for rich systems

In the regime of rich systems, as defined above, the X-ray-to-optical scaling is $L_X \propto L_s^{3.5}$. In this regime, for a Λ CDM cosmology, we found in §4 that

$$m \propto L_s^{1.5 \pm 0.26}. \quad (13)$$

This then implies that $m \propto L_X^{0.43 \pm 0.08}$. This is in good agreement with the analysis of Ledlow et al. (1999), who compared the observed XLF to PS mass functions and found $m \propto L_X^{0.4 \pm 0.03}$, in the bolometric X-ray band over the range $10^{41} < L_X / (\text{erg s}^{-1} h_{75}^{-2}) < 5 \cdot 10^{45}$ (solution Λ CDM2 in their Table 1 which is similar to the Λ CDM model adopted here.)

It is possible to compare this scaling with other cluster parameters such as velocity dispersion σ and temperature T . Under conditions of spherically-symmetric and isothermal equilibrium, the X-ray luminosity is connected to the velocity dispersion of the virialized halos by the relation $L_X \propto f^2 \sigma^3 T^{1/2}$ (Quintana & Melnick 1982), where f is the ratio of the gas mass to the total cluster mass. If the gas and galaxies are in hydrostatic equilibrium, the average plasma temperature is proportional to the depth of the cluster potential well ($T \propto \sigma^2$), leading to the following simple scaling relation $L_X \propto f^2 \sigma^4$. The observed $L_X - \sigma$ relation for clusters is not very far from this theoretical prediction. Several authors reported an empirical $L_X - \sigma$ relation close to $L_X \propto \sigma^4$ (Quintana & Melnick 1982; Mulchaey and Zabludoff 1998), while Xue & Wu (2000) and White, Jones & Forman (1997) derived somewhat steeper relations, $L_X \propto \sigma^{5.3 \pm 0.21}$ and $L_X \propto \sigma^{6.38 \pm 0.46}$, respectively.

Our results allow an alternative determination of this scaling relationship. Since our systems are defined by a fixed overdensity criterion, their typical size scales as $R_s \propto [\int_{L_{\text{min}}}^{\infty} L \Phi(L) dL]^{-1/3}$. Using eq. 5 of paper V and the cosmology dependent relation $m = L^\alpha$ we obtain,

$$L_s \propto \sigma^{\frac{6}{3\alpha-1}}. \quad (14)$$

Using the observed scaling relationship for the X-ray-to-optical luminosity ratio ($L_X \propto L_s^\beta$) we can write

$$L_X \propto \sigma^{\frac{6\beta}{3\alpha-1}} \quad (15)$$

For rich systems in the Λ CDM cosmology, this yields $L_s \propto \sigma^{1.7 \pm 0.38}$ which is in good agreement with the results of Schaeffer et al. (1993), who found $L_V \propto \sigma^{1.87 \pm 0.44}$ and those of Adami et al. 1998 who reported $L_{B_j} \propto \sigma^{1.56}$ with a large scatter.

In the X-ray band, our result would translate into the following scaling relation, $L_X = \sigma^{6 \pm 1.3}$, consistent with those found by Xue & Wu (2000) and White, Jones, & Forman (1997). In τ CDM cosmology we would have obtained

the following relations $L_s \propto \sigma^{3 \pm 0.13}$ and $L_X = \sigma^{10.5 \pm 1.3}$, in disagreement with the observations.

We can go a step further if we assume that clusters follow an isothermal relation $\sigma \propto T^{1/2}$ (which appears to be supported by the data of Ponman et al. 1996; White, Jones, & Forman 1997; Xue & Wu 2000). Inserting this $\sigma - T$ model into the $L_X - \sigma$ scaling relationship we obtain $L_X \propto T^{3 \pm 0.65}$. Again this result is in agreement with the fit of White, Jones, & Forman (1997) and Xue & Wu (2000).

Thus, in the regime of rich systems, the derived scalings are in agreement with the observations for the Λ CDM cosmology. For the τ CDM cosmology the agreement is poorer.

6.2. Scaling relations for poor systems

For poor systems, i.e. super- L_{gal}^* galaxies and poor groups, we found $L_X \propto L_s^{1.5}$. In this regime the mass-to-light ratio is nearly constant, $m \propto L_s^{1 \pm 0.1}$, for both Λ CDM and τ CDM cosmologies. This yields $L_X \propto L_s^{2.2 \pm 0.3}$, which, besides being in agreement with what we found, confirms in an independent way the bivariate scaling behavior of the optical-to-X-ray luminosity ratio over the group and cluster scales. Extending this analysis to velocity dispersions using 14, we derive a steep relationship $L_s \propto \sigma^{3 \pm 0.45}$. Now coupling our results with the observationally determined $L_X - L_s$ scaling relationship we obtain $L_X \propto \sigma^{3.9 \pm 1.2}$.

Because of the problems mentioned in §1, direct observational results for groups and poor clusters are much scattered, although they tend to lead to a flatter $L_X - \sigma$ relation compared to that of clusters. Mulchaey & Zabludoff (1998) obtain $L_X \propto \sigma^{4.3 \pm 0.4}$, Ponman et al. (1996) obtain $L_X \propto \sigma^{4.9 \pm 2.1}$, Helsdon & Ponman (2000) give $L_X \propto \sigma^{4.5 \pm 1.1}$, whilst Mahdavi et al. (1997) and Mahdavi et al. (2000) found much flatter relations, i.e. $L_X \propto \sigma^{1.56 \pm 0.25}$ and $L_X \propto \sigma^{0.4 \pm 0.3}$. The fit of Xue & Wu (2000) is intermediate in slope with $L_X \propto \sigma^{2.35 \pm 0.21}$. Our derived relation is consistent with the steep slopes and is marginally consistent with that of Xue & Wu.

Now if we assume $\sigma \propto T$ (Helsdon & Ponman 2000), we obtain the steeper relation $L_X \propto T^{3.9 \pm 1.2}$ which is in agreement with the theoretical predictions of Cavaliere, Menci & Tozzi (1997, 1999) (see the discussion at the end of the section) and in excellent agreement with the results $L_X \propto T^{4.9 \pm 0.9}$ of Helsdon & Ponman (2000).

If we had assumed a condition of virial equilibrium between condensed and diffuse baryons on the scale of groups, we would have obtained a flatter relation $L_X \propto T^{2.5}$ similar to the trend observed in clusters. Since this does not provide a good fit to data (see Fig. 9), we reinforce the conclusion of Ponman et al. that at the low end hierarchy of the clustering pattern, i.e. for low X-ray temperature systems, the virial equilibrium condition between galaxies and gas does not apply.

6.3. Discussion

The break in power-law scalings of mass, L_X , σ and T between rich and poor systems, occurring at $L_X \sim 10^{42} \text{ erg s}^{-1} h_{75}^{-1}$, has been noted by many authors. Here we have found that a change in the shape of the $L_X - L_s$ relation occurs at the same point.

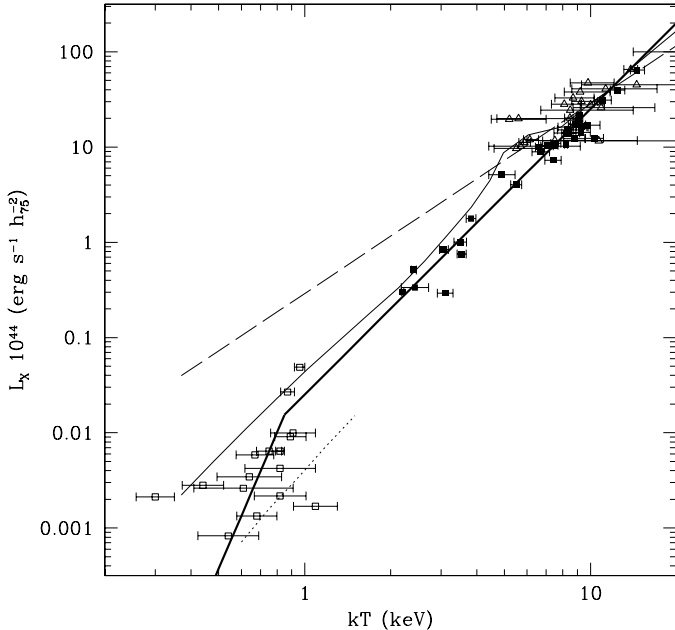


FIG. 9.— The relation between the bolometric luminosity and the temperature in Λ CDM cosmology. Data are from Arnaud & Evrard (1999) (filled squares), Allen & Fabian (1998) (triangles) and Ponman et al. (1996) (empty squares). The thick line refers to our predicted scaling behavior. The dashed line refers to the self-similar case and the solid line to predictions of the thermodynamic model of the $z = 0$ ICM (in a Λ CDM scenario) developed by Tozzi & Norman (1999) (the entropy excess is $K = 0.3 \cdot 10^{34} \text{ erg cm}^2 \text{ g}^{-5/3}$ constant with epoch and the cooling is included). The dotted line shows the relation $L_X - T$ at $z=0$ derived by Tozzi and Norman (1999) within the projected radius used in Ponman et al. (1996).

At a similar point there is a net change in the chemical properties and the spatial distribution of the ICM on the scales of groups (Renzini 1997, 1999). One might think that this is due solely to a change in the properties of the ICM. However, if the Λ CDM PS mass function is correct, then it is interesting that this transition corresponds to the same mass scale ($M_s \sim -23 + 5 \log h_{75}$) which separates efficient galaxy formation, with Υ low and approximately constant, from inefficient galaxy formation at which Υ begins to rise as $L_s^{0.5}$. This would suggest a connection between galaxy formation and the properties of the ICM. There are two proposed models for this connection. The star formation may have preheated the gas, or the low-entropy gas may have preferentially cooled into stars.

The broken power-law behavior is in quantitative agreement with predictions of the preheating scenario (Kaiser 1991, Evrard & Henry 1991) in which the entropy of the hot, diffuse intracluster medium is raised at early time (prior to gravitational collapse) by non-gravitational heating such as feedback effects of star formation, SN winds, shocks etc. Cavaliere, Menci, & Tozzi (1997, 1999) proposed a semi-analytic model of shocked ICM gas to explain the the observed $L_X - T$ relation. The same relation is reproduced by a model of Balogh et al. (1999) using the physics of an adiabatic isentropic collapse of a preheated gas. Both models make detailed predictions for the $L_X - T$ relations which are approximated by the power laws $L_X \propto T^5$ in the luminosity range $L_X < 0.25 \cdot 10^{44} (\text{erg s}^{-1} h_{75}^{-2})$ (groups) and $L_X \propto T^3$ in the

luminosity range $0.25 \cdot 10^{44} \leq L_X / (\text{erg s}^{-1} h_{75}^{-2}) \leq 5 \cdot 10^{44}$ (rich groups and clusters). Tozzi & Norman (2000) combine these two scenarios in a single model taking into account an initial entropy excess and the transition between the adiabatic and shock regime in the growth of X-ray halos. Their $L_X - T$ model and our predicted scalings are compared to data in Fig. 9.

On the other hand, the preferential cooling of low-entropy gas into stars in galaxies might also break the scaling (Thomas & Couchman 1992; Bryan 2000; Muanwong et al. 2001). For this process to explain the scaling, one requires greater efficiency of star formation for low-mass halos, e.g. 10% at $T \sim 1$ keV vs 4% at $T \sim 10$ keV (Bryan 2000). As discussed in §4, for the Λ CDM models, we found that the maximum star formation efficiency was as high as 25% for poor systems, about 2.5 times the global efficiency of 10%. For rich systems the star formation efficiency drops below the global average. Note that for a different mass spectrum, e.g. τ CDM there is no mass dependence of the star formation efficiency for high masses.

In summary, at least for the Λ CDM spectrum, it is interesting that the break in X-ray scaling properties occurs at roughly the same mass as the change in star formation efficiency. This suggests that there is a physical link between galaxy formation and the X-ray properties of the hot gas. Of course increased galaxy formation will lead to greater feedback as well as more efficient cooling of low-entropy gas, so it is difficult to distinguish between the scenarios discussed above.

7. SUMMARY AND CONCLUSIONS

We have used the B-band luminosity function of virialized systems to investigate scaling relations over a wide dynamic range of mass, from single galaxies to clusters of galaxies.

When our LF is compared to the Press-Schechter mass functions predicted in CDM cosmogonies we find that all these models fail, if a constant mass-to-light ratio is assumed. Specifically, in the τ CDM and Λ CDM models, the mass-to-light ratio must vary as $L^{-0.5}$ to match the faint-end of the luminosity function. On the other hand, a constant mass-to-light ratio and a ratio varying as $L^{0.5}$ match the bright ends of the τ CDM and Λ CDM models, respectively. For the Λ CDM model, the efficiency of star formation is maximized in the range of one to $\sim 5 L_{\text{gal}}^*$ or $10^{12.5}$ to $10^{13.5} h_{75}^{-1} m_{\odot}$, the regime of single galaxies and poor groups. In this range, the fraction of baryons is stars is $\sim 25\%$. The latter behavior of the mass-to-light ratio is in qualitative agreement with the predictions of recent semi-analytical models of galaxy formation, in which galaxy formation is inhibited by the reheating of cool gas on small-mass scales and by the long cooling times of hot gas on large-mass scales. The variation of the mass-to-light ratio with scale found by some authors through direct estimates of the masses of galaxy systems lends indirect support to the Λ CDM cosmology. A further test of the varying mass-to-light ratio model could be made via the comparison of observed peculiar velocities with the predictions from nearly all-sky optical galaxy catalogs such as the NOG.

Since our sample of galaxies is complete for objects

brighter than L_{gal}^* , we have also measured the halo occupation number. We find that, for Λ CDM models, this quantity grows more slowly than the total mass of the system, as required in the “halo” model of explain clustering.

Comparing X-ray luminosities as a function of optical luminosities in virialized systems, we find a break in the power-law slope of the relation as we go from groups to clusters, independent of the cosmological model. Dynamical scaling relations in X-ray systems are known to have break at a similar mass scale. Furthermore, the break occurs at a similar mass scale to that at which the mass-to-light ratio changes in the Λ CDM model. This suggests physical link between galaxy formation and the X-ray properties. However, these data cannot say whether this is due to reheating of the hot halo gas by supernovae or efficient cooling of low-entropy gas.

We look forward to forthcoming large field redshift sur-

veys planned with SDSS (Gunn & Knapp 1993), 2dF (Colless 1998), 2MASS (Huchra et al. 1998), which will (a) extend the range over which the system luminosity is determined (b) lower the luminosity threshold over which group members are selected and (c) reduce the errors in their distribution statistics. Moreover the DEEP2 redshift survey (Davis & Faber 1998) will probe the variation with cosmic time of the $M/L - L$, $L_X - L$ and $L - \sigma$ relations, allowing a deeper understanding of galaxy formation.

We wish to thank C. M. Baugh, A. J. Benson, M. Davis, R. Giovanelli, M. Haynes, P. Monaco, J. Newman, E. Scarnapiego, P. Tozzi, for interesting conversations. We are especially indebted to P. Tozzi who provided us results in advance of publication.

CM acknowledges the NSF grant AST-0071048, MJH acknowledges a grant from the NSERC of Canada.

REFERENCES

- Adami, C., Mazure, A., Biviano, A., & Katgert, P. 1998, *A&A*, 331, 493
- Allen, S. W. 1998, *MNRAS*, 296, 392
- Allen, S. W., & Fabian, A. C. 1998, *MNRAS*, 297, 57
- Balogh, M. L., Babul, A., & Patton, D. R. 1999, *MNRAS*, 307, 463
- Balogh, M. L., Christlein, D., Zabludoff, A. I., & Zaritsky, D. 2001, *astro-ph/0104042*
- Benson, A. J., Cole, S., Frenk, C. S., Baugh, C. M., & Lacey, C. G. 2000, *MNRAS*, 311, 793
- Benson, A. J. 2001, *MNRAS*, submitted, *astro-ph/0101278*
- Bond, J. R., & Efstathiou, G. 1984, *ApJ*, 285, L45
- Bond, J.R., Cole, S., Efstathiou, G., & Kaiser, N. 1991, *ApJ*, 379, 440
- Borgani, S., Gardini, A., Girardi, M., & Gottlober, S. 1997, *New Astronomy*, Vol. 2, 119
- Bower, R. G. 1991, *MNRAS*, 248, 332
- Bryan, G. L. 2000, *ApJ*, 544, 1
- Carlberg, R. G., Yee, H. K. C., Ellingson, E., Abraham, R., Gravel, P., Morris, S., & Pritchet, C. J. 1996, *ApJ*, 462, 32
- Cavaliere, A., & Fusco-Femiano, R. 1976, *A&A*, 49, 137
- Cavaliere, A., Colafrancesco, S., & Scaramela, R. 1991, *ApJ*, 380, 15
- Cavaliere, A., Menci, N., & Tozzi, P. 1997, *ApJ*, L21
- Cavaliere, A., Menci, N., & Tozzi, P. 1999, *MNRAS*, 308, 599
- Carlberg, R. G., Yee, H. K. C., Ellingson, E., Abraham, R., Gravel, P., Morris, S., & Pritchet, C. J. 1996, *ApJ*, 462, 32
- Cole, S., & Lacey, C. G. 1996, *MNRAS*, 281, 716
- Colless, M., M. 1998, in *XIV IAP Colloq. Wide Field Surveys in Cosmology*, ed. S. Colombi, Y. Mellier (Paris, Editions Frontieres), 77
- David, L. P., Jones, C., & Forman, W. 1996, *ApJ*, 473, 692
- Davis, M., & Faber, S. M. 1998 in *XIV IAP Colloq. Wide Field Surveys in Cosmology*, ed. S. Colombi & Y. Mellier (Paris, Edition Frontieres)
- Diaferio, A., Kauffmann, G., Colberg, J. M., & White, S. D. M. 1999, *MNRAS*, 307, 537
- Ebeling, H., Voges, W., Boehringer, H., & Edge, A.C., Huchra, J.P., & Briel, U.G. 1996, *MNRAS*, 281, 799
- Ebeling, H., Edge, A. C., Fabian, A. C., Allen, S. W., Crawford, C. S., & Boehringer, H. 1997, *ApJ*, 479, L101
- Ebeling, H., Edge, A. C., Boehringer, H., Allen, S. W., Crawford, C. S., Fabian, A. C., Voges, W., & Huchra, J.P. 1998, *MNRAS*, 301, 881
- Efstathiou, G., & Rees, M. J. 1988, *MNRAS*, 230, 5
- Eke, V. R., Cole, S., & Frenk, C. S. 1996, *MNRAS*, 282, 263
- Evrard, A. E., & Henry, J. P. 1991, *ApJ*, 383, 95
- Fukugita, M., Hogan, C. J., & Peebles, P. J. E. 1998, *ApJ*, 503, 518
- Girardi, M., Giuricin, G., Mardirossian, F., Mezzetti, M., & Boschin, W. 1998, *ApJ*, 505, 74
- Girardi, M., Borgani, S., Giuricin, G., Mardirossian, F., & Mezzetti, M. 2000, *ApJ*, 530, 62
- Giuricin, G., Marinoni, C., Ceriani, L., & Pisani, A. 2000, *ApJ*, 543, 178 (Paper III).
- Giuricin, G., Samurović, S., Girardi, M., Mezzetti, M., Marinoni, C., 2001, *ApJ*, 554, 857 (Paper IV)
- Governato, F., Babul, A., Quinn, T., Tozzi, P., Baugh, C. M., Katz, N., & Lake, G. 1999 *MNRAS*, 307, 949
- Gross, M. A. K., Somerville, R. S., Primack, J. R., Holtzman, J., & Klypin, A. 1998, *MNRAS*, 301, 81
- Gunn, J. E., & Knapp, G. R. 1993, in *ASP Conf. Ser. 43, Sky surveys: Protostars to Protogalaxies*, ed. B. T. Soifer (San Francisco: Astronomical Society of the Pacific), 267
- Helsdon, S. F., & Ponman, T. J. 2000, *MNRAS*, 315, 356
- Hickson, P., Mendes de Oliveira, C., Huchra, J. P., Palumbo, G.G.C. 1992, *ApJ*, 399, 353
- Huchra, J. P., Tollestrup, E., Schneider, S., Skrutski, M., Jarrett, T., Chester, T., Cutri, R. 1998, in *Highlights of Astronomy*, 11, 487.
- Hudson, M. J. 1993, *MNRAS*, 265, 43
- Hudson, M. J. 1994, *MNRAS*, 266, 475
- Jenkins, A., Frenk, C. S., Pearce, F. R., Thomas, P. A., Colberg, J. M., White, S. D. M., Colberg, J. M., Couchman, H. M. P., Peacock, J. A., Efstathiou, G., & Nelson, A. H. 1998, *ApJ*, 499, 20
- Jenkins, A., Frenk, C. S., White, S. D. M., Colberg, J. M., Cole, S., Evrard, A. E., & Yoshida, N. 2001, *MNRAS*, 321, 372
- Kaiser, N. 1991 *ApJ*, 383, 104
- Kauffmann, G., Colberg, J. M., Diaferio, A. & White, S. D. M. 1999, *MNRAS*, 303, 188
- Lacey, C., & Cole, S. 1993, *MNRAS*, 262, 627
- Lacey, C., & Cole, S. 1994, *MNRAS*, 271, 676
- Ledlow, M. J., Loken, C., Burns, J. O., Owen, F. N., & Voges, W. 1999, *ApJ*, 516, L53
- Lewis, A. D., Ellingson, E., Morris, S. L., & Carlberg, R. G. 1999, *ApJ*, 517, 587
- Mahdavi, A., Boehringer, H., Geller, M. J., Ramella, M. 1997, *ApJ*, 483, 68
- Mahdavi, A., Geller, M. J., Böhringer, H., Kurtz, M. J., & Ramella, M. 1999, *ApJ*, 518, 69
- Mahdavi, A., Boehringer, H., Geller, M. J., & Ramella, M. 2000, *ApJ*, 534, 114
- Marinoni, C., Monaco, P., Giuricin, G., & Costantini, B. 1998, *ApJ*, 505, 484 (Paper I)
- Marinoni, C., Monaco, P., Giuricin, G., & Costantini, B. 1999, *ApJ*, 521, 50 (Paper II)
- Marinoni, C. 2001a, Ph.D. Thesis, University of Trieste
- Marinoni, C., Giuricin, G., & Hudson, M. J., 2001b, *ApJ*, submitted (Paper V)
- Mo, H. J., & White, S. D. M., 1996, *MNRAS*, 282, 347
- Monaco, P. 1998 *Fund. Cosm. Phys.* 19, 153
- Moore, B., Frenk, C. S., & White S. D. M. 1993, *MNRAS*, 261, 827
- Muanwong, O., Thomas, P. A., Kay, S. T., Pearce, F. R., & Couchman, H. M. P. 2001, *ApJ*, 552, L27
- Mulchaey, J. S., & Zabludoff, A. I. 1998, *ApJ*, 496, 73
- Netterfield, C. B., et al. 2001, *ApJ* submitted (*astro-ph/0104460*)
- Neyman, J., Scott, E. L., & Shane, C. D. 1953, *ApJ*, 117, 92
- Park, C., Vogeley, M. S., Geller, M. J., Huchra, J. P. 1994, *ApJ*, 431, 569
- Peacock, J. A., & Smith, R. E., 2000, *MNRAS*, 318, 1144
- Ponman, T. J., Bourner P. D. J., Ebeling, H., Boehringer, H. 1996, *MNRAS*, 283, 690
- Press, W. H., & Schechter, P. 1974, *ApJ*, 187, 425
- Quintana, H., & Melnick, J. 1982, *AJ*, 87, 97
- Ramella, M., Pisani, A., & Geller, M. J. 1997, *AJ*, 113, 483
- Ramella, M. et al. 1999, *A&A*, 342, 1
- Renzini, A. 1997, *ApJ*, 488, 35

- Renzini, A. 1999, ESO Astrophysics Symposia *Chemical Evolution from Zero to High Redshift*, ed. J. Walsh & M. Rosa (Berlin: Springer)
- Scocimarro, R. ;, Sheth, R. K., Hui, L., & Jain, B. 2001, ApJ, 546, 20
- Salucci, P., & Persic, M. 1997, in ASP Conf. Ser. 117, *Dark and Visible Matter in Galaxies*, ed. M. Persic & P. Salucci (San Francisco: Astronomical Society of the Pacific), 1
- Schaeffer, R., Maurogordato, S., Cappi, A., & Bernardeau, F. 1993, MNRAS, 263, L21
- Schaeffer, R., & Silk, J. 1985, ApJ, 292, 319
- Schechter, P. 1976, ApJ, 203, 297
- Seljak, U. 2000, MNRAS, 318, 203
- Sheth, R. K., & Tormen, G. 1999, MNRAS, 308, 119
- Somerville, R. S., Lemson, G., Sigad, Y., Dekel, A., Kauffmann, G., & White, S. D. M. 2001, MNRAS, 320, 289
- Smail, I., Ellis, R. E., Dressler, A., Couch, W. J., Oemler, A., Sharples, R. M., & Butcher, H. 1997, ApJ, 479, 70
- Thomas, P. A. & Couchman, H. M. P. 1992, MNRAS, 257, 11
- Tozzi, P., & Norman, C. 2000, ApJ, submitted (astro-ph/0003289)
- White, D. A., Jones, C., & Forman W. 1997, MNRAS, 292, 419
- Xue, Y.-J. & Wu, X.-P., 2000, ApJ, 538, 65
- Zabludoff, A. I., & Mulchaey, J. S. 1998, ApJ, 496, 39
- Zucca, E. et al. 1997 1997, A&A, 326, 342

TABLE 1
 MASSES OF SYSTEMS FOR DIFFERENT MODELS

$M_s - 5 \log h_{75}$	$\frac{L_s}{L_\odot} h_{75}^2$	$\frac{m_s}{m_\odot} h_{75}$ (τ CDM)	$\frac{m_s}{m_\odot} h_{75}$ (Λ CDM)
-18	2.5×10^9	2.0×10^{12}	4.2×10^{11}
-19	6.2×10^9	3.5×10^{12}	8.2×10^{11}
-20	1.6×10^{10}	6.6×10^{12}	1.7×10^{12}
-21	3.9×10^{10}	1.3×10^{13}	3.7×10^{12}
-22	9.8×10^{10}	3.0×10^{13}	9.4×10^{12}
-23	2.5×10^{11}	7.6×10^{13}	3.0×10^{13}
-24	6.2×10^{11}	1.9×10^{14}	1.2×10^{14}
-25	1.6×10^{12}	4.8×10^{14}	5.1×10^{14}
-26	3.9×10^{12}	2.1×10^{15}	2.1×10^{15}